Crack Paths in Sharply Notched Specimens under In-Phase Biaxial Loadings

L. Susmel[1], D. Taylor[2] and R. Tovo[1]

[1] Department of Engineering - University of Ferrara
Via Saragat, 1 - 44100 Ferrara (Italy), e-mail: lsusmel@ing.unife.it, rtovo@ing.unife.it
[2] Department of Mechanical Engineering – Trinity College
Dublin 2 - Dublin (Ireland), e-mail: dtaylor@tcd.ie

ABSTRACT. *In this paper crack paths have been studied in sharply V-notched specimens subjected to in-phase mode I and II loadings. Specimen geometries allowed us to analyse the cracking behaviour in the presence of different ratios between mode I and II loadings. The investigated fatigue lives ranged from 10^3 up to $2\cdot 10^6$ cycles to failure. By studying the stress field along the measured crack paths, it has been observed that the role played by the shear stress was crucial up to a distance from the notch tip equal to L/2. Over this distance value, crack propagation was mainly mode I governed and the shear stress importance seemed to become secondary.*

INTRODUCTION

Understanding the cracking behaviour in the presence of fatigue loadings is a topical challenge for researchers engaged in fatigue problems both for predicting crack growth directions and for formulating fatigue criteria soundly connected to the experimental reality.

The present paper deals with the problem of making explicit a possible bridging between stress distributions along the crack paths and two criteria previously developed by the Authors to predict the fatigue limit of notched components. In particular, this paper reports the stress field analyses performed on the crack paths detected on V-notched specimens tested under in-phase mode I and II loadings.

In the past, we focused our attention on the fatigue limit estimation in the presence of stress concentrators subjected to biaxial loadings [1]. This problem has been addressed by using two different approaches [1, 2]: at the beginning, it has been extended the critical distance method (CDM) [3] to multiaxial fatigue situations and, subsequently, the Susmel and Lazzarin multiaxial fatigue criterion [4] has been applied reinterpreted in terms of the critical distance mechanics. In particular, the line method (LM) of Taylor [3] and the modified Wöhler curve method (MWCM) of Susmel and Lazzarin [4] demonstrated to be capable of fatigue limit predictions within an error interval of about ±15% [2]. LM method has been applied in the following form:

$$\frac{1}{2L}\int_0^{2L}\sigma_{\theta,a}dr = \sigma_0 \quad (1)$$

where $\sigma_{\theta,a}$ was the amplitude of the stress component perpendicular to the direction, emanating from the notch tip, which experienced the maximum range of the normal stress, σ_0 was the fully-reversed plain fatigue limit and L was the El Haddad's short crack constant defined as [5]:

$$L = \frac{1}{\pi}\left(\frac{\Delta K_{th}}{\Delta\sigma_0}\right)^2 \quad (2)$$

The MWCM has been applied as:

$$\tau_a + \left(\tau_0 - \frac{\sigma_0}{2}\right)\frac{\sigma_{n,max}}{\tau_a} \le \tau_0 \quad (3)$$

where τ_a and $\sigma_{n,max}$ were the shear stress and the maximum normal stress relative to the plane of maximum shear stress amplitude passing through the point positioned along the notch bisector at a distance from the notch tip equal to L/2. Here σ_0 and τ_0 were the fully-reversed plain uniaxial fatigue limit and the fully-reversed plain torsional fatigue limit, respectively.

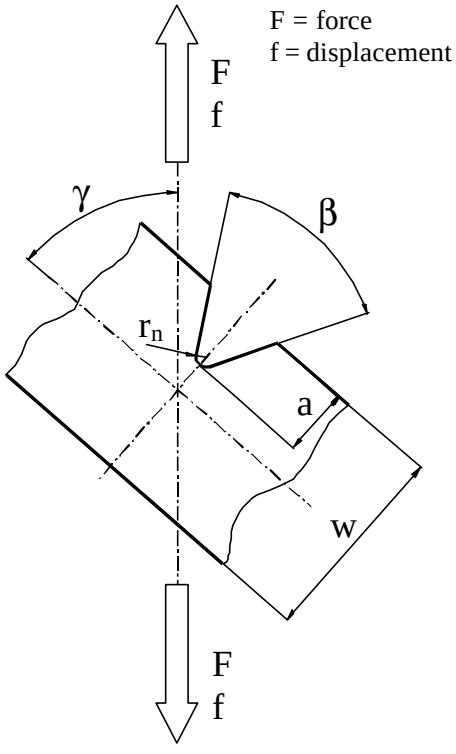

Figure 1. Notch geometry and symbolism.

In the present paper, stress fields along the measured crack paths have been studied systematically to form some hypotheses capable of explaining the reason both methods work even though the CDM is based on a mode I governed fatigue damage, whereas the MWCM is a crack initiation criterion.

EXPERIMENTAL DETAILS

The material employed in the present study was BS 040A12 low carbon steel, having the following mechanical properties: tensile strength σ_T=410 MPa, fully-reversed axial fatigue limit σ_0=273 MPa, fully-reversed torsional fatigue limit τ_0=171 MPa and El Haddad's short-crack constant L=0.2 mm. In-phase mode I and mode II loadings have been generated by using specimens having geometries directly derived from the compact tension-shear specimens [1, 2]. In our samples cracks were substituted for V-shaped notches having a nominal opening angle of 60°.

In order to obtain different ratios between mode I and II stress components, the γ angle (fig. 1) has been changed, using values of 90°, 60° and 45°, respectively. Lastly, the scale effect has been study by testing two different specimen widths for every considered γ angle value: in the first sample type a was 3mm and w was 6mm and in the second one they were 5mm and 10mm, respectively.

Fully reversed fatigue tests have been performed by using an INSTRON 8501 fatigue test machine. Test frequency was equal to 30 Hz and fatigue failure was defined by 50% axial stiffness drop.

In order to measure the crack growth directions, the zone ahead of the notch tip has been polished and crack paths have been measured by using a LEICA MEF4M microscope with a JVC TK-C1380 digital camera. Pictures and measurments have been managed by using the *A4i Docu* software.

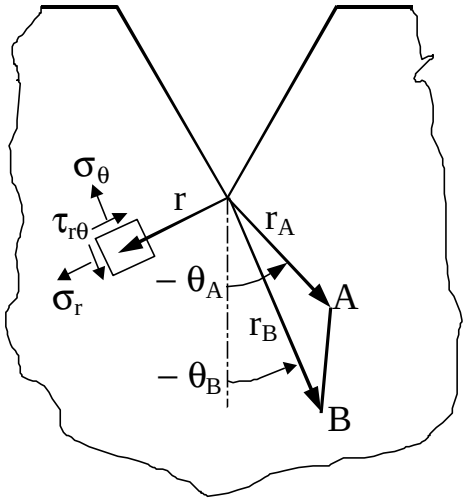

Figure 2. Crack path schematisation.

CRACK PATHS AND STRESS FIELDS

Crack propagations have been followed up to a distance from the notch tip equal to 3L=0.6mm (point B, fig. 2). When cracks changed their direction inside the investigated area, paths have been schematised as two straight lines. The position of both point A and B has been defined by using the polar co-ordinates r and θ, as sketched in fig. 2. We assumed that cracks always initiated at the notch tip, even if it was not always true. In fact, in some cases fatigue cracks initiated at different points positioned along the notch tip circumference. Unfortunately, close to the notch tip, the material microstructure was too damaged by the crack propagation phenomenon. This situation was a consequence of the adopted failure criterion, which allowed us to stop tests only when the crack had grown up to a length of about a quarter of the gross width, w. For this reason it was not possible to accurately determine the position of the crack initiation point.

Linear-elastic stress fields along the measured crack paths have been studied by using the ANSYS software, without modelling the crack. This assumption takes as its starting point the idea that, when the crack is not so long, the stress distribution in the crack propagation volume is mainly influenced by the presence of the notch [7]. All the analyses have been done by considering a notch root radius of 0.074mm.

Fatigue results and measured crack paths are summarised in Table 1, where the reported values refer to: specimen code, γ_a; values of the specimen dimensions (see fig. 1 for symbol definitions); amplitude of the applied force, F_a; number of cycles to failure, N_f, and run outs; polar co-ordinates describing the crack paths, r and θ. Finally, the last three columns report the ρ ratio between the shear stress, $\tau_{r\theta}$, and the normal

stress, σ_θ, calculated at r=L/2, the θ_{LM} angle value maximising the fatigue damage calculated according to the LM, eq. (1), and the θ_ρ angle giving the direction that minimised the $|\rho|$ value.

As example, in fig. 3 it has been reported, one for each tested specimen configuration, the picture of the crack path, with a magnification of 10X, and the stress field, determined by the FE analyses, in terms of stress normal and tangential to the crack propagation straight lines. The plotted stress fields have been determined by FEs under the maximum value of the applied force.

Sp. Code	**a** [mm]	**r_n** [mm]	**r_n/a**	**β** [°]	**w** [mm]	**F_a** [kN]	**N_f** [Cycles]	**Run Out**	**θ_A** [°]	**r_A** [mm]	**θ_B** [°]	**r_B** [mm]	**r**	**θ_{LM}** [°]	**θ_r** [°]
90_05_1	4.92	0.075	0.015	57° 28'	10.05	2.50	33060		-19.2	0.384	-31.4	0.6	0.34		
90_05_2	5.02	0.081	0.016	57° 32'	10.1	1.80	2000000	X				0.6			
90_05_3	5.16	0.072	0.014	57° 32'	10.15	2.50	46888				-22.5	0.6	0.29		
90_05_4	5.06	0.031	0.006	57° 28'	10.15	2.20	127582				-47.9	0.6	0.05	-38.2	-29.2
90_05_5	5.17	0.081	0.016	57° 33'	10	2.00	574377		-41.3	0.506	-46.7	0.6	0.03		
90_05_6	4.95	0.075	0.015	58° 04'	10.05	1.90	607433		-39.4	0.370	-48.5	0.6	0.06		
90_05_8	5.09	0.064	0.013	57° 08'	10.15	1.90	992992		46.1	0.436	50.4	0.6	25.00		
90_03_1	2.93	0.071	0.024	56° 24'	6.1	1.75	19046		-21.9	0.271	-19.5	0.6	2.00		
90_03_2	2.96	0.066	0.022	56° 51'	6.1	1.55	35288		29.3	0.545	28.0	0.6	3.34		
90_03_4	3.03	0.088	0.029	57° 25'	6.05	1.00	1660181		48.7	0.171	35.7	0.6	3.34		
90_03_5	3.11	0.035	0.011	57° 46'	6.1	1.00	1405877		41.7	0.504	43.3	0.6	12.50	-39.1	-30.3
90_03_6	2.93	0.07	0.024	57° 03'	6.1	1.10	479980		59.8	0.477	54.9	0.6	12.50		
90_03_8	2.92	0.154	0.053	57° 03'	6.05	1.20	462696		50.1	0.370	44.7	0.6	2.50		
90_03_9	3.02	0.078	0.026	57° 05'	6.1	1.10	840286		62.4	0.532	51.2	0.6	0.91		
60_05_1	4.89	0.073	0.015	57° 12'	10.15	2.50	52749		-21.0	0.572	-22.9	0.6	0.07		
60_05_2	5.08	0.081	0.016	57° 64'	10.1	2.50	47024		-31.3	0.264	-49.1	0.6	0.04		
60_05_3	4.99	0.068	0.014	57° 22'	10.1	1.90	340645		-31.9	0.218	-26.7	0.6	0.05		
60_05_4	4.82	0.076	0.016	57° 38'	10.1	1.90	369109		-42.0	0.462	-45.5	0.6	0.16		
60_05_5	4.79	0.079	0.016	57° 31'	10.1	1.65	2077381		-48.1	0.266	-52.2	0.6	0.23	-25.0	-16.8
60_05_6	5.12	0.088	0.017	57° 13'	10.1	1.75	659765				-51.3	0.6	0.26		
60_05_7	5.06	0.083	0.016	57° 08'	10.15	1.65	575553				-55.3	0.6	0.31		
60_05_8	4.92	0.075	0.015	57° 18'	10.1	1.75	745632		-36.9	0.155	-54.9	0.6	0.14		
60_05_9	5.03	0.068	0.014	57° 56'	10.1	1.65	534420		-43.8	0.157	-53.4	0.6	0.18		
60_03_1	3.01	0.065	0.022	57° 21'	5.8	1.20	173467		-16.8	0.358	-30.0	0.6	0.08		
60_03_2	3.02	0.073	0.024	57° 58'	5.75	1.00	674133		-40.1	0.308	-49.6	0.6	0.17		
60_03_3	2.99	0.082	0.027	57° 62'	5.93	1.00	552233				-51.2	0.6	0.29		
60_03_4	2.98	0.081	0.027	57° 05'	5.88	1.20	365249		-28.5	0.213	-49.6	0.6	0.04		
60_03_5	2.98	0.088	0.03	57° 18'	5.8	0.90	2000000	X				0.6		-24.3	-16.3
60_03_6	3.06	0.091	0.03	57° 43'	5.82	0.95	994062		-50.5	0.315	-54.1	0.6	0.29		
60_03_7	2.88	0.078	0.027	57° 09'	5.93	0.95	1568092		-52.0	0.220	-56.7	0.6	0.30		
60_03_8	2.82	0.079	0.028	57° 33'	6.01	1.45	53815		-30.0	0.428	-34.8	0.6	0.06		
60_03_9	3.11	0.072	0.023	57° 61'	5.95	1.45	63742		-14.2	0.495	-18.5	0.6	0.11		

Table 1. (Caption on next page)

Sp. Code	a [mm]	r_n [mm]	r_n/a	β [°]	w [mm]	F_a [kN]	N_f [Cycles]	Run Out	θ_A [°]	r_A [mm]	θ_B [°]	r_B [mm]	r	θ_{LM} [°]	θ_r [°]
45_05_1	5.00	0.073	0.015	57° 13'	10.2	2.00	614898		-28.9	0.086	-45.5	0.6	0.21		
45_05_2	4.99	0.069	0.014	57° 59'	10.3	2.50	164588		-5.3	0.136	-31.2	0.6	0.20		
45_05_3	5.01	0.054	0.011	57°03'	10.3	1.80	1572192				-50.6	0.6	0.29		
45_05_4	4.97	0.071	0.014	57° 54'	10.15	2.00	1627475		-57.6	0.358	-55.1	0.6	0.37		
45_05_5	5.1	0.079	0.015	57° 06'	10.15	2.50	291357		-55.5	0.260	-57.9	0.6	0.34	-22.1	-14.5
45_05_6	5.08	0.068	0.013	57° 12'	10.05	1.80	1338746				-48.0	0.6	0.26		
45_05_7	4.98	0.072	0.014	57° 21'	10.25	3.00	56444		-33.0	0.412	-33.5	0.6	0.09		
45_05_8	5.11	0.067	0.013	57° 18'	10.2	2.00	1067819				-50.8	0.6	0.29		
45_05_9	5.02	0.069	0.014	57° 07'	10.1	3.00	38131				-32.4	0.6	0.09		
45_03_1	3.08	0.071	0.023	57° 32'	3.1	1.75	32770		-55.0	0.199	-36.4	0.6	0.40		
45_03_2	2.98	0.068	0.023	57° 43'	3.2	1.60	54433		0.0	0.466	-6.0	0.6	0.17		
45_03_3	2.94	0.082	0.028	57° 19'	2.9	1.20	349054				-47.8	0.6	0.31		
45_03_4	2.98	0.091	0.031	57° 22'	2.95	1.00	1212560				-44.9	0.6	0.29		
45_03_5	3.03	0.055	0.018	57° 12'	2.95	1.20	602101		-20.1	0.205	-40.4	0.6	0.03	-15.8	-9.9
45_03_6	2.94	0.076	0.026	57° 13'	3.05	1.00	1535352		-41.6	0.160	-49.9	0.6	0.25		
45_03_7	3.05	0.077	0.025	57° 19'	3.05	1.10	1115318		-40.3	0.331	-47.9	0.6	0.24		
45_03_8	3.08	0.073	0.024	57° 38'	2.95	1.10	551675				-45.6	0.6	0.29		

Table 1. Specimen dimensions, fatigue test results and measured crack paths.

DISCUSSION

As it can be observed from Table 1, crack paths were, in general, characterised by θ_A and θ_B values less the zero. Only the 90_03 configuration (and the specimen named 90_05_08) showed crack paths having $\theta_{A,B}>0$. Unfortunately, it was not possible to explain this anomalous behaviour just by using the stress field distributions.

In order to classify the crack growth modes, we assumed that propagation could be considered as mode I governed when the ratio $\rho=\tau_{r\theta}/\sigma_\theta$ was less than 0.2.

Appart form the 90_03 configuration, cracks always tended to propagate along directions which were able to minimise the shear stress contribution. In fact, as showed by Table 1, when r>L/2, the ρ ratio was, in general, less than about 0.2 and it decreased as r increased (because normal stresses tended to be greater than zero, whereas shear stresses approached a value very close to zero). Therefore, experimental evidences suggest that, when r>L/2, the shear stress influence played a secondary role. At this point, it can be formed the hypothesis that the material was capable of knowing a priori the direction characterised, after a certain distance from the notch tip depending on the material mecanichal properties, by a prevailing mode I fatigue damage. An interesting consequence of this situation is that crack propagation directions seem to be more influenced by the stress field distribution outside the Neuber's structural volume than by that happens very close to the notch tip. Moreover, comparing the ρ value and the number of cycles to failure, it can be observed that, in general, the ρ ratio increased as

N_f increased. It could suggest that the shear stress influence on the crack propagation disappeared sooner in the low/medium than in the high cycle fatigue regime.

In any case, shear stress was never negligible up to a distance from the notch tip equal to L/2. Thus, it can be formed the hypothesis that L/2 is the transition point between a crack growth under mixed modes (r<L/2) and a crack propagation mainly mode I governed (it held true especially in the high cycle fatigue regime).

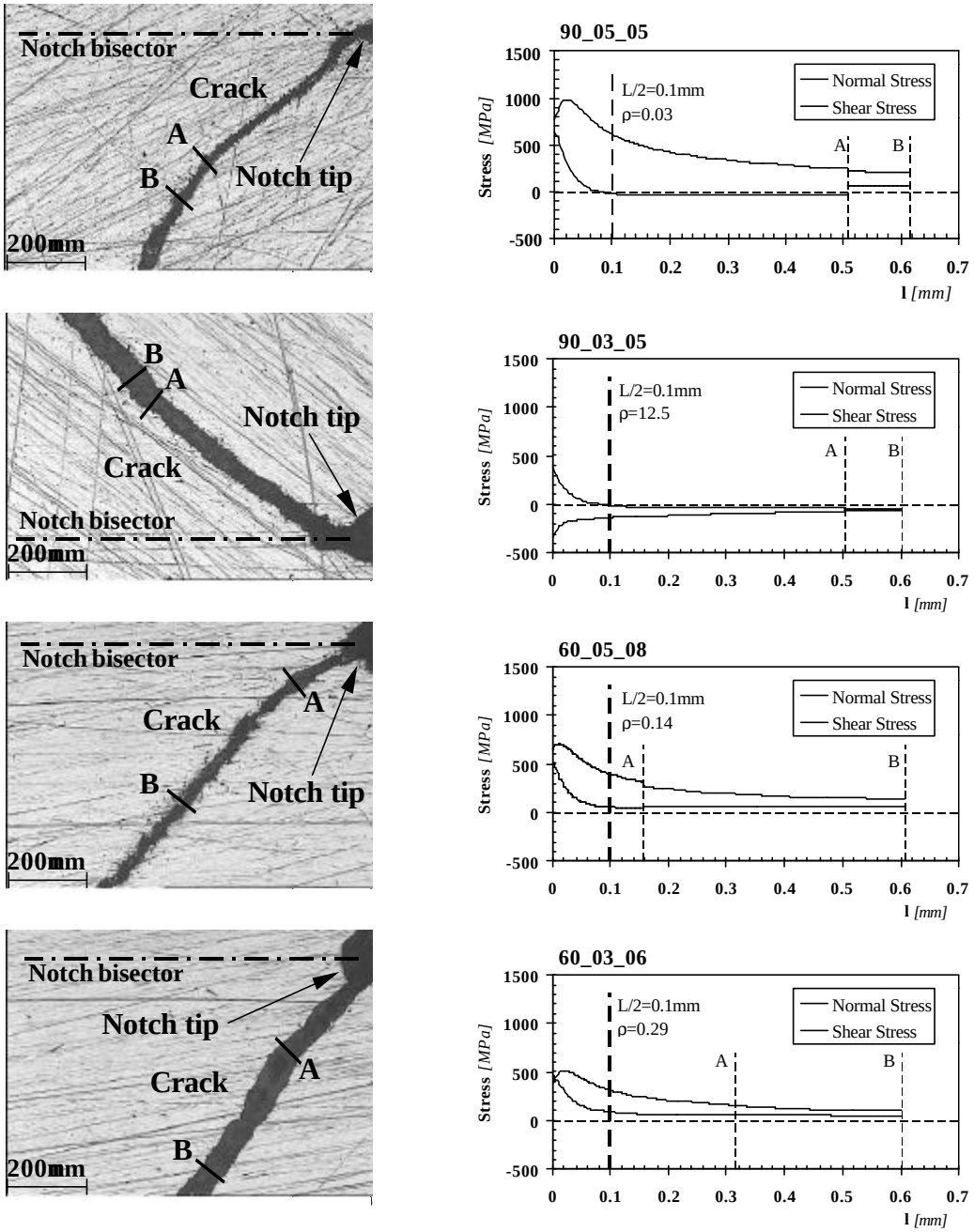

Figure 3. (Caption on next page)

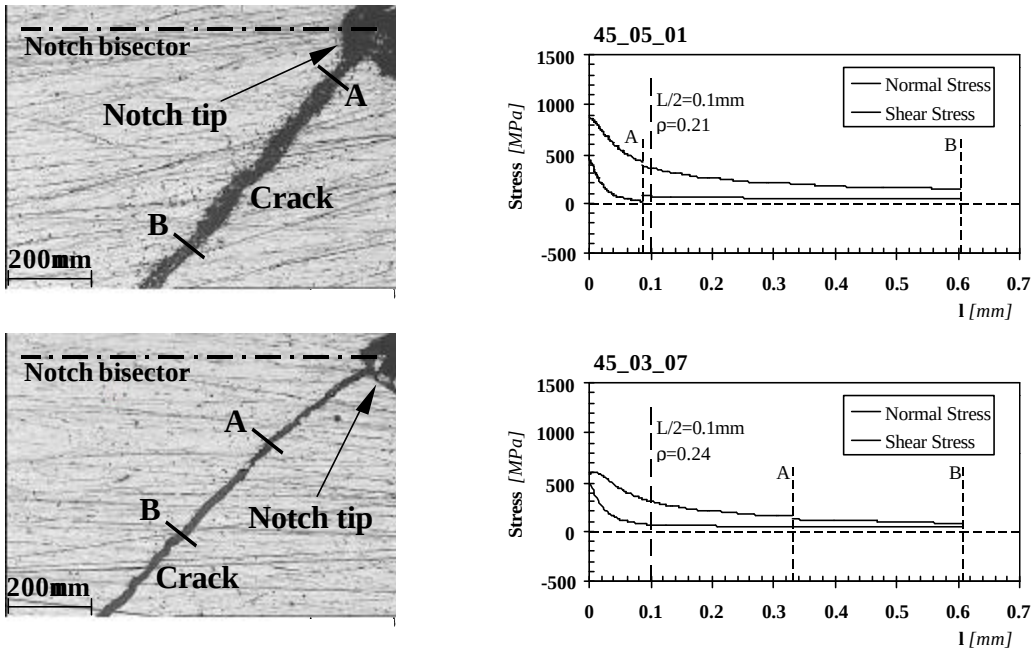

Figure 3. Pictures of crack paths (10X magnification) and stress distributions along the crack propagation directions.

This idea seems to be partially supported by the last column of Table 1: the direction minimising the ρ parameter has θ_ρ values close to the measured $\theta_{A,B}$ angles. In other words, an ideal crack path could be schematised as a straight line experiencing an initial stage I (mainly mode II dominated) up to r=L/2 and a successive stage II characterised by a propagation mainly mode I governed.

All the considerations reported above could even use to give a physical explanation of the correspondence, in terms of stresses, we found between the CDM and the MWCM and published elsewhere [2]. In fact, the MWCM seems to better model the crack initiation, which depends on the mixed mode stress field very close to the notch tip. On the contrary, the LM is a mode I based criterion, which is capable of predicting the formation of a mode I non-propagating crack [6]. Therefore, the MWCM seems to better interpret the physical situation up to r=L/2, that is, it is capable of quantifying the fatigue damage that creates the condition for the crack formation (stage I). On the contrary, the LM is soundly connected to the reality by predicting the formation of a mode I fatigue crack. The last statement is strongly supported by the θ_{LM} values listed in Table 1: in general, the orientation of the direction characterised by the maximum fatigue damage according to the LM are close to those observed experimentally.

Moreover, both the MWCM and the LM are coherent even in terms of stresses used for the fatigue limit estimations. In fact, applying the MWCM at a distance r=L/2, the prediction is performed by considering a multiaxial situation, which is crucial up to the point where stress calculations are made. On the contrary, averaging the normal stress along the direction which experiences the maximum normal stress, as postulated by the

LM, the fatigue damage parameter does not take into account the shear stress contribution, but this contribution plays an important role up to a distance equal only to one quarter of the integration path length.

As pointed out above, the 90_03 configuration showed a completely different behaviour compared to the one discussed in the previous paragraphs. In fact, $\theta_{A,B}$ angles were always greater than zero. In this situation, FE analyses highlighted that a mixed mode propagation was always present up to r=L/2. Over this distance, normal stresses tended to a value approaching zero, whereas shear stress to a value different from zero. Unfortunately, it is not possible to interpret this behaviour just by using the stress field distributions. Nevertheless, for this kind of specimens the MWCM continues to be meaningful, because it models the biaxial stress fields close to the notch tip, but the LM is no more connected to the physical reality, because cracks did not grow along the direction experiencing the maximum normal stress.

Finally, it is important to highlight that it was very difficult to explain the crack direction change only in terms of stresses. In any case, apart from the 90_03 configuration, when cracks changed their direction an important increase of the shear stress was never introduced.

CONCLUSIONS

1. The performed experimental tests demonstrated that in the presence of in-phase mixed mode loadings cracks propagate along directions which, outside the Neuber's structural volume, experience the maximum range of the normal stress;
2. Up to a distance equal to L/2 stress fields along the crack paths are biaxial, and the shear stress influence can not be neglected;
3. Over a distance equal to L/2 crack propagation is mainly mode I governed and the shear stress contribution plays a secondary role;
4. The MWCM demonstrated to be capable of quantifying the multiaxial fatigue damage that brings the formation of the fatigue crack, but it is not suitable for predicting the crack path direction;
5. The LM demonstrated to be capable of modelling the mode I cracking behaviour outside the Neuber's structural volume, with the advantage of giving important information on the crack propagation directions;

REFERENCES

1. Susmel, L., Taylor, D. (2002) In: *FATIGUE 2002*, Blom, A. (Ed.), 1889-1897.
2. Susmel, L., Taylor, D. (2003) Submitted to: *Fatigue Fract. Engng. Mater. Struct.*
3. Taylor, D. (1999) *Int. J. Fatigue* **21**, 413-420.
4. Susmel, L., Lazzarin, P. (2002) *Fatigue Fract. Engng. Mater. Struct.* **25**, 63-78.
5. El Haddad, M. H., Dowling, N. F., Topper T. H., Smith, K. N. (1980) *Int. J. Fract.* **16**, 15–24.
6. Taylor, D. (2002) *Fatigue Fract. Engng. Mater. Struct.* **24**, 215–224.
7. Lazzarin, P., Zambardi R. (2001) *Int. J. of Fracture* **112**, 275-298.